Available online at www.sciencedirect.com
SCIENCE DIRECT®
Journal of Organometallic Chemistry 682 (2003) 26–34
Journal of Organometallic Chemistry
www.elsevier.com/locate/jorganchem

Bridged 3,5-disubstituted pyrazolate ligands as support of metallomesogens containing $[Pd(\eta^3\text{-}C_3H_5)]^+$ fragments X-ray crystal structure of $[Pd(\eta^3\text{-}C_3H_5)(\mu\text{-}pz^{R2})]_2\cdot CH_2Cl_2$ ($R = C_6H_4OC_{12}H_{25}$). Part III☆

M.C. Torralba [a], M. Cano [a,*], S. Gómez [a], J.A. Campo [a], J.V. Heras [a], J. Perles [b], C. Ruiz-Valero [b]

[a] Facultad de Ciencias Químicas, Departamento de Química Inorgánica I, Universidad Complutense, E-28040 Madrid, Spain
[b] Instituto de Ciencia de Materiales, CSIC, Cantoblanco, E-28049 Madrid, Spain

Received 28 March 2003; accepted 28 April 2003

Abstract

The mesomorphic properties of two new long-chain 3,5-(4-*n*-alkoxyphenyl)pyrazoles Hpz^{R2} ($R = C_6H_4OC_nH_{2n+1}$, $n = 16$, 18) have been studied and compared with those of related compounds containing shorter chains ($n = 4$, 6, 8, 10, 12, 14). For liquid crystal purposes, the derivative with 14 carbon atoms in the chain behaves as the best compound on the basis of the lowest melting point and the widest stability range of the mesophases. New Pd(II) complexes of formula $[Pd(\eta^3\text{-}C_3H_5)(\mu\text{-}pz^{R2})]_2$ ($R = C_6H_4OC_nH_{2n+1}$, $n = 8$, 10, 12, 14, 16, 18) (**1**–**6**) containing the mesomorphic ligands as pyrazolate-bridging groups have been prepared and characterised. In solution, three conformational isomers (two symmetric and one asymmetric corresponding to different orientations of the allyl groups) have been found. In the solid state, the X-ray crystal structure of **3** ($n = 12$) evidenced the asymmetric isomer. The structure shows a bowlic core drawn on the basis of the boat-like conformation of the six-membered ring $Pd(NN)_2Pd$. However, a rod-like shape could also be considered by taking the molecular dimensionality into account (47.80 Å in length × 4.75 Å in wide). The Pd-complexes **2**–**6** were found to have liquid crystal properties exhibiting enantiotropic smectic phases consistent with the molecular characteristics. Moreover, the molecular packing of **3** is described as the layer-like type in which the molecules are parallel to the *c*-axis but tilted off the layer, this fact appearing similar to the molecular ordering in the smectic fluid phases.
© 2003 Elsevier B.V. All rights reserved.

Keywords: Long-chained 3,5-disubstituted pyrazoles; Mesomorphic behaviour; Palladium–pyrazolate complexes; X-ray structure; Calamitic Pd(II) complexes

1. Introduction

Metal-containing liquid crystals are an increasing area of research which has been commonly developed on compounds having rod-like or disk-like shapes [1–4]. By contrast, metallomesogens with bowl-shaped structures have been scarcely investigated [5–9].

Dinuclear bisazolate metal derivatives are among the complexes extensively characterised with a boat-like conformation defined by two metal centres and two azolate-bridging groups [10–15]. In this context, since the pioneering studies of Trofimenko [16], some allylpyrazolatepalladium derivatives have been investigated, and the X-ray structures of two of them $[Pd(\eta^3\text{-}C_3H_5)(\mu\text{-}pz^{R2})]_2$ ($R = CH_3$, CF_3) have been reported [17,18]. The mentioned complexes showed the characteristic boat-like Pd_2N_4 core which gave rise to a bowlic molecular shape.

On the other hand, in a previous work we have reported the mesomorphic behaviour of a series of 3,5-

☆ For Parts I and II, see Refs. [19] and [20].

* Corresponding author. Fax: +34-91-3944352.
E-mail address: mmcano@quim.ucm.es (M. Cano).

0022-328X/03/$ - see front matter © 2003 Elsevier B.V. All rights reserved.
doi:10.1016/S0022-328X(03)00669-7

disubstituted pyrazoles Hpz^{R2} containing long-chain 4-*n*-alkyloxyphenyl substituents ($R = C_6H_4OC_nH_{2n+1}$, $n = 4$, 6, 12, 14) [19]. By contrast, from these ligands, the related Rh-complexes of the types $[Rh(\mu\text{-}pz^{R2})(CO)_2]_2$ or $[RhCl(CO)_2(Hpz^{R2})]$ ($R = C_6H_4OC_nH_{2n+1}$, $n = 4$, 6, 8, 10, 12, 14) did not exhibit liquid crystal properties [19], as it also occurred for the homologues $[RhCl(CO)_2(Hpz^{R})]$ ($R = C_6H_4OC_nH_{2n+1}$, $n = 4$, 6, 8, 10) containing the non-mesomorphic 3(5)-substituted pyrazoles Hpz^{R} [20]. Because Rh-fragments had been proved to be useful as polar groups to induce mesomorphism [3,4,21,22], the absence of liquid crystal properties on our Rh-derivatives was attributed to their inadequate molecular skeletal characteristics. In fact, we proved that when we prepared straight molecules *t*-$[PdCl_2(Hpz^{R})_2]$ ($R = C_6H_4OC_nH_{2n+1}$, $n = 6$, 8, 10, 12, 14, 16, 18) with enough length to width relationship, they behave as calamitic materials in agreement with their molecular shape [23], although the metallic influence should not be discarded.

In order to explore the influence of the metal core on the mesomorphic behaviour of pyrazolate derivatives, new complexes containing the $[Pd(\eta^3\text{-}C_3H_5)]^+$ fragment have been prepared. The main goal was directed towards the evaluation of the ability of rod-like ligands to induce mesomorphism on a bowlic core.

The current report presents the results of complexes of the type $[Pd(\eta^3\text{-}C_3H_5)(\mu\text{-}pz^{R2})]_2$ ($R = C_6H_4OC_nH_{2n+1}$, $n = 8$, 10, 12, 14, 16, 18) (**1**–**6**) (Scheme 1) which, with the exception of **1**, were found to have liquid crystals properties at difference of the related non-mesogens $[Rh(\mu\text{-}pz^{R2})(CO)_2]_2$ [19].

The mesomorphic behaviour of these Pd-complexes as well as of the two new pyrazole ligands Hpz^{R2} ($R = C_6H_4OC_nH_{2n+1}$, $n = 16$, 18) ($\mathbf{L^{C16}}$, $\mathbf{L^{C18}}$) (Scheme 1) has been analysed.

2. Experimental

2.1. Materials and physical measurements

All commercial reagents were used as received. The starting Pd-complex $[Pd(\mu\text{-}Cl)(\eta^3\text{-}C_3H_5)]_2$ was purchased from Sigma-Aldrich and used as received.

The 4-*n*-alkyloxyacetophenone and ethyl 4-*n*-alkyloxybenzoate derivatives were synthesised by alkylation of 4-hydroxyacetophenone or ethyl 4-hydroxybenzoate, respectively, with the corresponding *n*-alkyliodide in acetone solution of potassium carbonate as previously described for related compounds [20,24,25]. All these compounds were characterised satisfactorily by analytical and spectroscopic techniques.

Elemental analyses for carbon, hydrogen and nitrogen were carried out by the Microanalytical Service of the Complutense University. IR spectra were recorded on an FTIR Nicolet Magna-550 spectrophotometer with samples as KBr pellets in the 4000–400 cm^{-1} region.

^{1}H-NMR spectra were performed on a Varian VXR-300 or on a Bruker DPX-300 spectrophotometers of the NMR Service of the Complutense University from solutions in $CDCl_3$. Chemical shifts δ are listed in ppm relative to TMS using the signal of the deuterated solvent as reference, and coupling constants J are in hertz. Multiplicities are indicated as s (singlet), d (doublet), t (triplet), and m (multiplet). The atomic numbering used in the assignment of the NMR signals is shown in Scheme 1. The ^{1}H chemical shifts and coupling constants are accurate to 0.01 ppm and 0.3 Hz, respectively.

Phase studies were carried out by optical microscopy using an Olympus BX50 microscope equipped with a Linkam THMS 600 heating stage. The temperatures

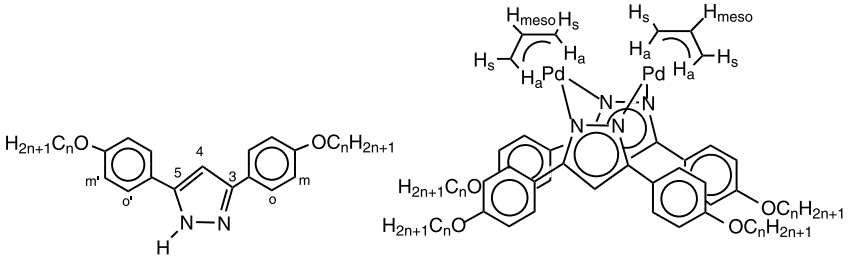

LIGANDS Hpz^{R2}		*COMPLEXES* $[Pd(\eta^3\text{-}C_3H_5)(\mu\text{-}pz^{R2})]_2$
$\mathbf{L^{C8}}$	*n= 8*	**1**
$\mathbf{L^{C10}}$	*n= 10*	**2**
$\mathbf{L^{C12}}$	*n= 12*	**3**
$\mathbf{L^{C14}}$	*n= 14*	**4**
$\mathbf{L^{C16}}$	*n= 16*	**5**
$\mathbf{L^{C18}}$	*n= 18*	**6**

Scheme 1.

were assigned on the basis of optic observations with polarised light.

Measurements of the transition temperatures were made using a Perkin–Elmer Pyris 1 differential scanning calorimeter with the sample (2–6 mg) hermetically sealed in aluminium pans and with a heating or cooling rate of 5–10° min^{-1}.

2.2. Synthetic methods

2.2.1. Preparation of Hpz^{R2} ($R = C_6H_4OC_nH_{2n+1}$, $n = 16, 18$) ($\mathbf{L^{C16}}$, $\mathbf{L^{C18}}$)

These new pyrazol ligands were prepared following a similar procedure to that described for related pyrazoles with shorter chains [19,25]. Due to the low solubility of the new pyrazoles in relation to those with shorter chains, several recrystallisation processes in dichloromethane–hexane or chloroform–hexane were required.

$\mathbf{L^{C16}}$: Yield: 83%. Elemental analyses: Found: C, 80.2; H, 10.6; N 3.8. Calculated for $C_{47}H_{76}N_2O_2$: C, 80.5; H, 10.9; N, 4.0%. IR (KBr, cm^{-1}): ν(NH) 3431, ν(CN) 1615. $\mathbf{L^{C18}}$: Yield: 75%. Elemental analyses: Found: C, 80.5; H, 10.9; N, 3.3. Calculated for $C_{51}H_{84}N_2O_2$: C, 80.9; H, 11.2; N, 3.7%. IR (KBr, cm^{-1}): ν(NH) 3423, ν(CN) 1614.

^{1}H-NMR ($CDCl_3$) δ: 7.64d (Ho, $J = 8.8$ Hz), 6.96d (Hm, $J = 8.8$ Hz), 6.69s (H4), 4.00t (OCH_2, $J = 6.0$ Hz), 1.80–1.20m ($-(CH_2)_n-$), 0.88t (CH_3, $J = 7.0$ Hz) ppm.

2.2.2. Preparation of $[Pd(\eta^3\text{-}C_3H_5)(\mu\text{-}pz^{R2})]_2$ ($R = C_6H_4OC_nH_{2n+1}$, $n = 8, 10, 12, 14, 16, 18$) (**1**–**6**)

To a solution of $[Pd(\mu\text{-}Cl)(\eta^3\text{-}C_3H_5)]_2$ (0.15 mmol) and the corresponding pyrazole (0.30 mmol) in dry THF (15 ml) under nitrogen atmosphere was added dropwise an excess of NEt_3 (2 ml) or a slight excess of 60% NaH. The mixture of reaction was stirred at room temperature approximately 3 h. The mixture was then filtered over Celite to eliminate some metallic palladium formed by decomposition. The obtained solution was left at low temperature, giving rise to a white solid which was filtered off and dried in vacuo (yield: 35–50%).

1 ($n = 8$): Elemental analyses: Found: C, 65.2; H, 7.5; N, 4.3. Calculated for $C_{68}H_{96}N_4O_4Pd_2$: C, 65.5; H, 7.8; N, 4.5%. IR (KBr, cm^{-1}): ν(CN) 1612. **2** ($n = 10$): Elemental analyses: Found: C, 66.8; H, 8.1; N, 4.1. Calculated for $C_{76}H_{112}N_4O_4Pd_2$: C, 67.2; H, 8.3; N, 4.1%. IR (KBr, cm^{-1}): ν(CN) 1612. **3**·$\mathbf{CH_2Cl_2}$ ($n = 12$): Elemental analyses: Found: C, 65.4; H, 8.4; N, 3.6. Calculated for $C_{84}H_{128}N_4O_4Pd_2\cdot CH_2Cl_2$: C, 65.6; H, 8.4; N, 3.6%. IR (KBr, cm^{-1}): ν(CN) 1614. **4** ($n = 14$): Elemental analyses: Found: C, 70.1; H, 9.2; N, 3.5. Calculated for $C_{92}H_{144}N_4O_4Pd_2$: C, 69.8; H, 9.2; N, 3.5%. IR (KBr, cm^{-1}): ν(CN) 1613. **5**·$\frac{1}{2}\mathbf{CH_2Cl_2}$ ($n = 16$): Elemental analyses: Found: C, 69.2; H, 9.1; N, 3.3. Calculated for $C_{100}H_{160}N_4O_4Pd_2\cdot\frac{1}{2}CH_2Cl_2$: C, 69.5; H, 9.3; N, 3.2%. IR (KBr, cm^{-1}): ν(CN) 1614. **6** ($n = 18$): Elemental analyses: Found: C, 71.9; H, 9.6; N, 3.1. Calculated for $C_{108}H_{176}N_4O_4Pd_2$: C, 71.8; H, 9.8; N, 3.1%. IR (KBr, cm^{-1}): ν(CN) 1613.

As expected, the NMR data of all Pd-complexes are similar. Therefore, only those of **1** are given as representative example.

1 ($n = 8$): ^{1}H-NMR ($CDCl_3$) δ: symmetric isomer: 8.06–7.90m (Ho), 7.04–6.96 (Hm), 6.65s (H4), 5.05m (H$meso$), 2.97d (Hs, $J = 6.6$ Hz), 2.50d (Ha, $J = 12.4$ Hz), 4.05t (OCH_2, $J = 6.4$ Hz), 1.90–1.20m ($-(CH_2)_6-$), 0.90t (CH_3, $J = 6.6$ Hz) ppm. Asymmetric isomer: 8.06–7.90m (Ho), 7.04–6.96 (Hm), 6.60s (H4), 5.05m (H$meso$), 3.26d (Hs, $J = 6.6$ Hz), 2.87d (Hs, $J = 6.6$ Hz), 2.37d (Ha, $J = 12.2$ Hz), 2.04d (Ha, $J = 12.7$ Hz), 4.05t (OCH_2, $J = 6.4$ Hz), 1.90–1.20m ($-(CH_2)_6-$), 0.90t (CH_3, $J = 6.6$ Hz) ppm. Symmetric isomer: 8.06–7.90m (Ho), 7.04–6.96 (Hm), 6.55s (H4), 5.05m (H$meso$), 3.16d (Hs, $J = 6.6$ Hz), 1.93 (Ha, partially overlapped with the CH_2 protons), 4.05t (OCH_2, $J = 6.4$ Hz), 1.90–1.20m ($-(CH_2)_6-$), 0.90t (CH_3, $J = 6.6$ Hz) ppm. Isomer ratio: ca. 7:9:3.

2.3. X-ray structure determination

Colourless crystals of $[Pd(\eta^3\text{-}C_3H_5)(\mu\text{-}pz^{R2})]_2\cdot CH_2Cl_2$ ($R = C_6H_4OC_{12}H_{25}$) (**3**) were obtained from dichloromethane–hexane solution. A summary of the conditions for data collection is given in Table 1. Suitable prismatic crystals of this compound were resin epoxy coated and mounted on a Bruker Smart CCD diffractometer equipped with a normal focus, 2.4 kW sealed tube X-ray source (Mo–K_α radiation, $\lambda = 0.71073$ Å) operating at 40 kV and 20 mA. Data were collected over a hemisphere of reciprocal space by a combination of three sets of exposures. Each set had a different φ angle for the crystal and each exposure of 20 s covered 0.3° in ω. Unit cell dimensions were determined by a least-squares fit of 40 reflections with $I > 2\sigma(I)$ and $4° < 2\theta < 46°$. The first 30 frames of data were recollected at the end of the data collection to monitor crystal decay, and no appreciable decay was observed.

The structure was solved by Patterson methods and refined in the triclinic space group $P\bar{1}$. Full-matrix least-squares refinement with anisotropic thermal parameters for all non-H atoms was carried out by minimising $w(F_0^2 - F_c^2)^2$. The largest residual peak in the final difference map was 0.49 e $Å^{-3}$, near the C83 atom. The refinement converged to an R value of 0.067.

All calculations were performed using: SMART software for data collection; SAINT for data reduction [27], SHELXTL™ to resolve and refine the structure and to

Table 1
Crystal and refinement data for $[Pd(\eta^3\text{-}C_3H_5)(\mu\text{-}pz^{R2})]_2\cdot CH_2Cl_2$ (R = $C_6H_4OC_{12}H_{25}$) (**3**)

Empirical formula	$C_{84}H_{128}N_4O_4Pd_2\cdot CH_2Cl_2$
Formula weight	1555.63
Crystal system	triclinic
Space group	$P\bar{1}$
Unit cell dimensions	
a (Å)	10.0(1)
b (Å)	17.0(2)
c (Å)	28.2(3)
α (°)	90.0(2)
β (°)	87.9(2)
γ (°)	90.0(2)
V (Å^3)	4788(80)
Z	2
T (K)	293(2)
$F(0\,0\,0)$	1652
ρ_{calc} (g cm^{-3})	1.079
μ (mm^{-1})	0.474
Crystal dimensions (mm^3)	0.30 × 0.15 × 0.08
Scan technique	ω scans
Data collected	(−9, −16, −28) to (9,14,25)
θ range (°)	3.23–20.81
Reflections collected	13 391
Independent reflections	8645 (R_{int} = 0.096)
Data/restraints/parameters	8645/0/879
Observed reflections [$I > 2\sigma(I)$]	3618
GOF on F^2	0.814
R [a]	0.067
Rw_F [b]	0.138

[a] $\Sigma|\Delta F|/\Sigma|F_o|$.
[b] $\Sigma[w(\Delta F)^2]/\Sigma[w(F_o)^2]$.

prepare material for publication [28], and ATOMS for molecular graphics [29].

Different crystals of **3** were used to solve the X-ray structure. However in all cases the same structural results, corresponding to the asymmetric isomer, were observed (see below Section 3.2).

3. Results and discussion

3.1. Synthetic and characterisation studies

The 3,5-di(4-*n*-hexadecyloxyphenyl)pyrazole ($\mathbf{L^{C16}}$) and 3,5-di(4-*n*-octadecyloxyphenyl)pyrazole ($\mathbf{L^{C18}}$) have been synthetised by an analogous procedure to that reported for related pyrazoles [19,26,30,31], and fully characterised by spectroscopic and analytical techniques (see Section 2).

The reaction of $[Pd(\mu\text{-}Cl)(\eta^3\text{-}C_3H_5)]_2$ in tetrahydrofuran with two equivalents of pyrazolate ligand (pz^{R2}), prepared in situ by deprotonation of Hpz^{R2} with NaH or NEt_3 in the same solvent, yields to the dimeric complexes $[Pd(\eta^3\text{-}C_3H_5)(\mu\text{-}pz^{R2})]_2$ (R = $C_6H_4OC_nH_{2n+1}$, n = 8, 10, 12, 14, 16, 18) (**1**–**6**). The analytical and spectroscopic data agree with the proposed formulation (see Section 2). The ^{1}H-NMR spectra of the complexes were consistent with the presence of a series of eight doublets, four in the range 1.90–2.50 ppm (J ca. 12 Hz) and other four between 2.95 and 3.30 ppm (J ca. 7 Hz), and a multiplet at ca. 5.05 ppm, corresponding to the *anti*, *syn* and *meso* protons of the allyl group, respectively. In addition, three singlets for the H4 protons of the pyrazolate ligand were observed at ca. 6.65, 6.60 and 6.55 ppm. This behaviour agrees with the presence of three conformational isomers (two symmetric and one asymmetric) corresponding to those containing both allyl groups pointing in (isomer a), out (isomer b) or in and out (isomer c) towards the metallic core of the Pd_2N_4 boat (Fig. 1).

It was interesting to note that in the original work on dinuclear Pd(II) allylpyrazolate derivatives reported by Trofimenko [16], a mixture of the related isomers had already been proposed for $[Pd(\eta^3\text{-}CH_2C(CH_3)CH_2)(\mu\text{-}pz^{Me2})]_2$, on the basis of the presence of four types of *syn* and four of *anti* protons, and for $[Pd(\eta^3\text{-}C_3H_5)(\mu\text{-}pz^{Me2})]_2$, from very complex *syn* and *anti* multiplets besides four methyl peaks.

In our complexes, the eight very well-resolved doublets of the *syn* and *anti* protons of the allyl group, four for the asymmetric and the other four from the two symmetric isomers, as well as the three H4 proton signals of the pyrazolate ligand allowed us to identify undoubtedly the presence of the three isomers and suggest that no exchange among them should occur at room temperature. The ^{1}H-NMR spectra in C_6D_6 in the 25–70° range showed broadening of all signals with the temperature. At 70°, the H4 protons are observed close to coalescence as well as the *syn* and *anti* protons are also close to equivalence. Therefore, a fluxional behaviour of complexes yielding a rapid isomeric interchange is suggested on heating.

The proton ratios indicated that the major isomer in the mixture at room temperature was the asymmetric one, being the relative areas among them of ca. 7:9:3.

3.2. Crystal structure of $[Pd(\eta^3\text{-}C_3H_5)(\mu\text{-}pz^{R2})]_2\cdot CH_2Cl_2$ (R = $C_6H_4OC_{12}H_{25}$) (3)

Suitable crystals of **3** were obtained from dichloromethane–hexane. Fig. 2a illustrates the molecular structure with the atom numbering scheme, and Table 2 lists selected bond distances and angles. The complex crystallises in the $P\bar{1}$ space group with two $[Pd(\eta^3\text{-}C_3H_5)(\mu\text{-}pz^{R2})]_2$ unities and two dichloromethane molecules in the unit cell. No short contacts between them are observed. The geometry about the Pd(II) atoms is slight distorted square-planar with the Pd1 and Pd2 0.38(1) and 0.30(1) Å out of their coordination planes (N1N3C80C82 and N2N4C83C85, respectively).

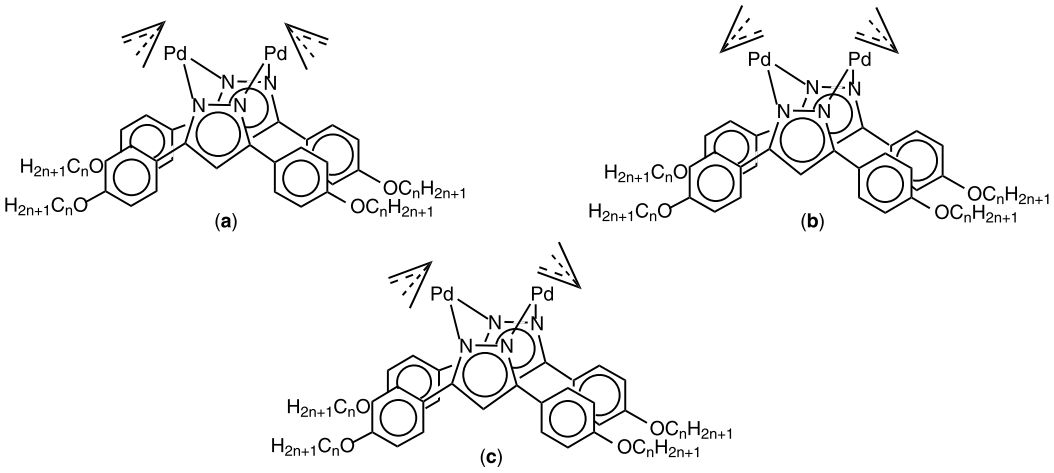

Fig. 1. Conformational isomers for $[Pd(\eta^3\text{-}C_3H_5)(\mu\text{-}pz^{R2})]_2$.

The allyl groups, C80C81C82 and C83C84C85, deviate from the ideal allyl geometry (C–C distances of ca. 1.36 Å and C–C–C angles of 120°). So, each allyl group presents two types of C–C distances of ca. 1.40 and 1.28 Å and a C–C–C angle of ca. 151°. Similar distorted allyl groups have also been found in other complexes containing $[Pd(\eta^3\text{-allyl})]^+$ fragments [32–35].

The main structural feature was that related with the molecular central core, which adopts a bowl-shaped structure, as expected. The bowl is determined by two

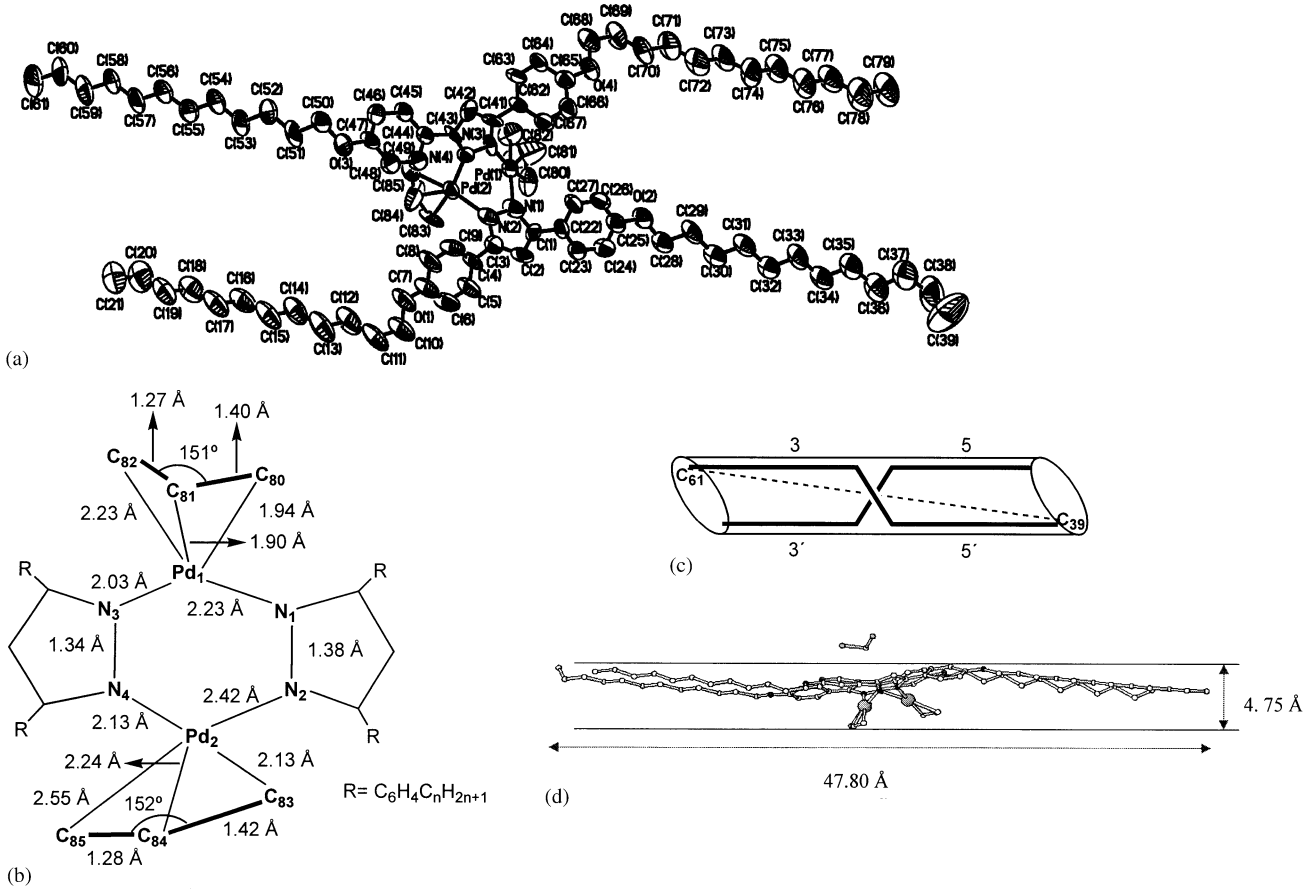

Fig. 2. (a) Perspective ORTEP plot of **3**. Hydrogen atoms and solvent molecule have been omitted for clarity, and thermal ellipsoids are at 50% probability level. (b) Molecular schematic representation of the asymmetric isomer showing bond lengths and angles. (c) Schematic representation of the distorted 'H' shape, showing the numbering of the chains on the pyrazolate rings. (d) View of **3** showing the bowl-shaped core and including its length to width dimensionality.

Table 2
Selected bond distances (Å) and angles (°) for $[Pd(\eta^3\text{-}C_3H_5)(\mu\text{-}pz^{R2})]_2 \cdot CH_2Cl_2$ ($R = C_6H_4OC_{12}H_{25}$) (**3**)

Bond distances (Å)	
Pd1–N1	2.23(2)
Pd1–N3	2.03(2)
Pd1–C80	1.94(2)
Pd1–C81	1.90(2)
Pd1–C82	2.23(3)
C80–C81	1.40(3)
C81–C82	1.27(3)
Pd1···Pd2	3.293
Pd2–N2	2.42(2)
Pd2–N4	2.13(2)
Pd2–C83	2.13(2)
Pd2–C84	2.24(2)
Pd2–C85	2.55(2)
C83–C84	1.42(2)
C84–C85	1.28(2)
Bond angles (°)	
N1–Pd1–N3	102.7(7)
N1–Pd1–C80	91.6(9)
N1–Pd1–C82	167.9(5)
N3–Pd1–C80	165.7(6)
N3–Pd1–C82	89.4(7)
C80–Pd1–C82	76.3(9)
C80–C81–C82	151(3)
N2–Pd2–N4	91.1(7)
N2–Pd2–C83	102.2(8)
N2–Pd2–C85	169.5(4)
N4–Pd2–C83	166.1(5)
N4–Pd2–C85	99.3(7)
C83–Pd2–C85	67.3(8)
C83–C84–C85	152(2)

palladium atoms and the four nitrogens of two pyrazolate rings bridging the metal centers. Then the six-membered ring $Pd(NN)_2Pd$, in which the N1–Pd1–N3 and N2–Pd2–N4 planes intersect with an angle of 83.2(7)°, generates a boat-like conformation. The openess of the bowl is primarily determined by the N1–Pd1–N3 and N2–Pd2–N4 angles which were 102.7(7)° and 91.1(7)°, respectively. The flat pyrazolate rings further extend the size of the bowl spreading out upwards to make the top of the bowl. The $C_6H_4OC_{12}H_{25}$ substituents spread out sideways forming an almost flat plane.

Each pyrazolate ligand carries two alkyloxyphenyl chains in the 3- and 5-positions having both phenyl groups almost coplanar (12.9(8)° and 15.0(7)°) but twisted from their own pyrazolate ring angles with values ranging from 36.8(8)° to 46.6(7)°. Because the dihedral angle between planes containing the pyrazolate-bridging groups is 46.6(7)°, the corresponding phenyl groups of different pyrazolates form dihedral angles from 28.1(7)° to 42.7(7)°.

The Pd···Pd distance in the boat is 3.293 Å similar to that found in $[Pd(\eta^3\text{-}C_3H_5)(\mu\text{-}pz^{R2})]_2$ ($R = CH_3$, CF_3) (3.343 and 3.2169 Å, respectively) [17,18], indicating the slight incidence of sterically demanding substituents $C_6H_4OC_{12}H_{25}$ on the metal core. It was also observed for other parameters involved in the boat. So, the Pd–N bond lengths were 2.03(2) and 2.23(2) Å for Pd1 and 2.13(2) and 2.42(2) Å for Pd2 (Fig. 2b), slightly longer that those for $[Pd(\eta^3\text{-}C_3H_5)(\mu\text{-}pz^{R2})]_2$ ($R = CH_3$, CF_3) (2.067–2.083 and 2.101–2.111 Å, respectively) [17,18], and the intersection angles between the two Pd–N–N–Pd planes were 113.6(6)° for **3**, and 103.2° and 106.6° for $[Pd(\eta^3\text{-}C_3H_5)(\mu\text{-}pz^{R2})]_2$ ($R = CH_3$, CF_3) [17,18].

The other relevant structural feature of **3** is concerned with the conformational isomer found which was associated with the asymmetric one, according to the major isomer detected in solution. So, the Pd–C distances involving the terminal atoms of the allyl group were 2.23(3) and 1.94(2) Å for Pd1 and 2.13(2) and 2.55(2) Å for Pd2, whereas those with the central carbon atom were 1.90(2) and 2.24(2) Å respectively (Fig. 2b). The asymmetric isomer was also proposed by Trofimenko [16] for some pyrazolate derivatives and found for $[Pd(\eta^3\text{-}C_3H_5)(\mu\text{-}pz^{CF3})]_2$ from the X-ray crystal structure [18].

An interesting result emerges by considering the whole molecular geometry. The molecule presents a distorted 'H' form with the four chains almost parallel but those on the same side of the pyrazolate groups (3 and 3′, and 5 and 5′; see Fig. 2c) slightly shifted. Then the diagonal line linking the terminal carbon atoms of opposite chains (3 and 5′) is longer than that from 3′ and 5, and so the molecule presents a very elongated shape with the distance between C39 and C61 of 47.80 Å being extremely long related to the width of 4.75 Å (determined by the distance between two parallel planes containing the C80 and C48 atoms, respectively) (Fig. 2d).

The molecular packing is recovered in Fig. 3. It could be described as layer-like type with the layers formed by stacking of two sheets of molecules with opposite orientation. Each sheet in turns has molecules with the same orientation and presents interdigitation between neighbours. Because of the molecular shape, the layers adopt a zigzag or folded structure.

However by considering the molecule as rod-like type, the structure suggests an ordering in which all the molecules are approximately parallel to the *c*-axis (Fig. 2d), but taking as molecular axis the longest distance of 47.80 Å corresponding to the C39–C61 diagonal mentioned above the molecules are deviated 10° from the layer. This ordering suggests some resemblance with the layered molecular organisation observed in the smectic mesophases.

3.3. Thermal studies

The thermal behaviour of the Pd-complexes **1**–**6** as well as the two new pyrazoles Hpz^{R2} ($R = C_6H_4OC_nH_{2n+1}$, $n = 16$, 18) ($\mathbf{L^{C16}}$, $\mathbf{L^{C18}}$) was studied

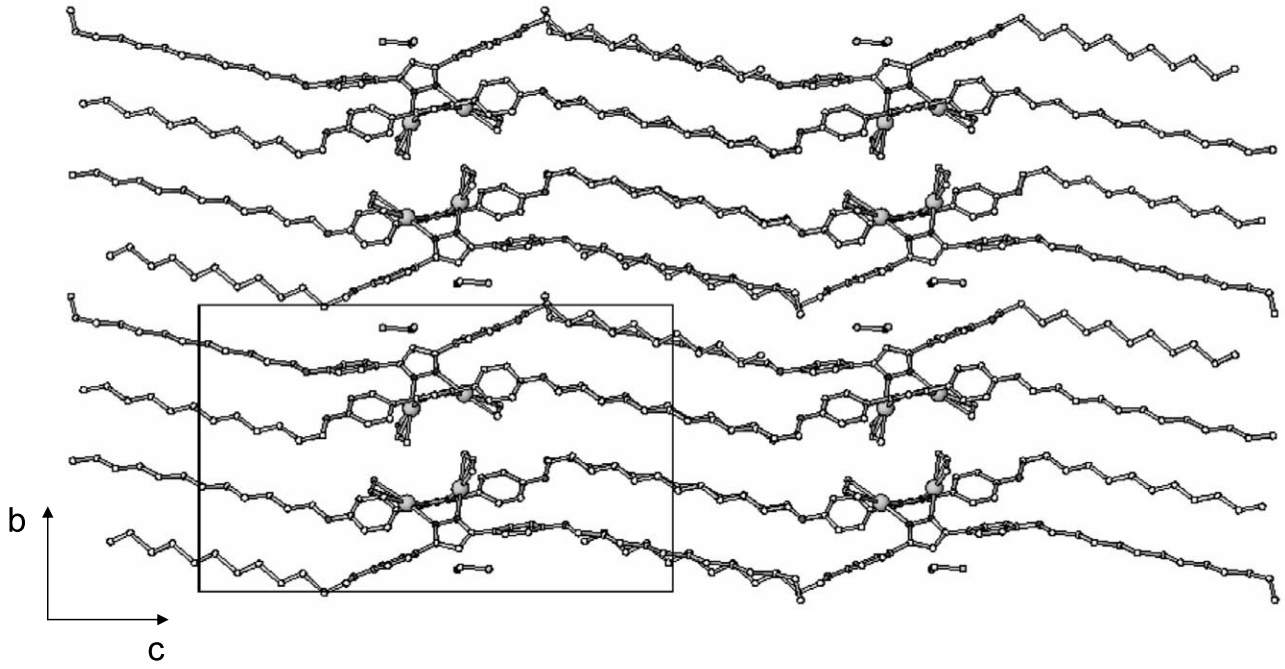

Fig. 3. Molecular packing of **3** along the *c*-axis.

by polarised light microscopy and differential scanning calorimetry.

The two new pyrazole ligands behave as liquid crystals like the related counterparts Hpz^{R2} previously described containing side chains with 4 ($\mathbf{L^{C4}}$), 6 ($\mathbf{L^{C6}}$), 8 ($\mathbf{L^{C8}}$), 10 ($\mathbf{L^{C10}}$), 12 ($\mathbf{L^{C12}}$) and 14 ($\mathbf{L^{C14}}$) carbon atoms [19,25]. $\mathbf{L^{C16}}$ and $\mathbf{L^{C18}}$ exhibit enantiotropic smectic C mesophases at lower transition temperatures and over a narrower temperature range as it was observed by polarised light microscopy ($\mathbf{L^{C16}}$: Cr, 111 °C; SmC, 151 °C I; $\mathbf{L^{C18}}$: Cr, 115 °C. SmC, 147 °C I). Fig. 4 displays a bar graph showing the phase behaviour of all of those ligands for comparative purposes. A decrease in the melting temperature accompanying an increase in the side chain length is observed from $\mathbf{L^{C4}}$ to $\mathbf{L^{C14}}$, while $\mathbf{L^{C16}}$ and $\mathbf{L^{C18}}$ show the opposite behaviour. The stability range displayed by the mesophases was also found to be dependent on the number of carbon atoms in the side chains and following the same sequence, i.e.

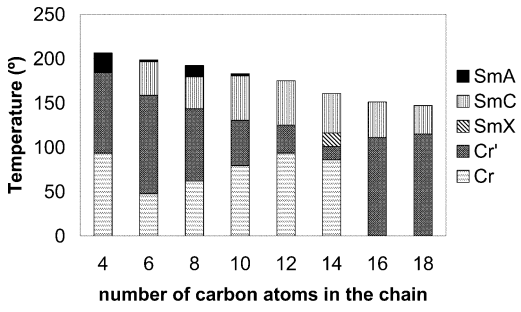

Fig. 4. Bar graph showing the thermal behaviour of the Hpz^{R2} compounds.

increasing from $\mathbf{L^{C4}}$ to $\mathbf{L^{C14}}$ and then lowering for $\mathbf{L^{C16}}$ and $\mathbf{L^{C18}}$. Then it is of interest to note that for liquid crystal purposes, the best ligand was $\mathbf{L^{C14}}$ which gives a lower melting point at 100 °C and also shows a wider mesophase stability range of 60 °C. This fact merits further comment. The chains contribute to the structural anisotropy but because they do not easily pack in the crystalline form they act to reduce the melting point (until a determined chain length). That is, it should exist a compromise between the increase of the chain length and the disorder produced by them.

The Pd-complexes **1**–**6**, with the exception of that with the shortest chain **1**, exhibited enantiotropic smectic phases at temperatures between 43 °C and 108 °C, which were smectic A for **2**, smectic A and smectic C for **3** and smectic C for **4**–**6**. Table 3 lists the onset temperatures observed for these compounds on the cooling. The melting temperature varied between 43 °C and 60 °C and the clearing temperatures were in the range 95–108 °C. For this class of complexes, it was observed that the increase of the number of carbon atoms of the alkyloxy chains does not introduce significant modifications on the melting and clearing points. Fig. 5 shows the textures of the mesophases of compounds **2**–**4** as representative examples.

In relation to the mesogenic free ligands [19,26], it can be observed that the corresponding pyrazolate Pd-complexes show liquid crystal phases at lower temperatures.

The comparison of the mesomorphic properties on the Pd-complexes $[Pd(\eta^3\text{-}C_3H_5)(\mu\text{-}pz^{R2})]_2$ with the non-mesomorphism of the related Rh-derivatives [Rh(μ-

Table 3
Phase properties of compounds **1**–**6** determined by DSC on cooling [a]

	Transition	T (°C)	ΔH (kJ mol^{-1})
1	I → Cr	124.9	−31.7
2	I → SmA	107.5	−10.4
	SmA → Cr	ca. 60	[b]
3	I → SmA	95.8	−21.0
	SmA → SmC	77.1	−0.4
	SmC → Cr	43.5	[c]
4	I → SmC	101.7	−12.9
	SmC → Cr	58.6	−56.7
5	I → SmC	98.5	−4.8
	SmC → Cr	46.9	[c]
6	I → SmC	95.5	−9.6
	SmC → Cr	61.3	−55.5

[a] Onset temperatures are given. If heating temperatures are used, melting and clearing points appear overlapped in a broad peak. By contrast they were clearly observed using the cooling data and agree with the visual observations by microscopy.
[b] Observed only by polarised light microscopy.
[c] It is not possible to determine the enthalpy variation of this transition because it is in the low limit of the calorimeter.

$pz^{R2})(CO)_2]_2$ [19] suggests some comments. This behaviour could be due to a lower symmetry of the Pd-complexes resulting from the different orientation of the allyl groups on the molecule (see Section 3.1). The reduced molecular symmetry should give rise to a less favourable packing in the solid state reducing the corresponding melting points. In agreement with this proposal, the observed melting points of the Rh-complexes $[Rh(\mu\text{-}pz^{R2})(CO)_2]_2$ ($R = C_6H_4OC_nH_{2n+1}$) of 143.8 °C, 133.4 °C and 126.0 °C for $n = 10$, 12, 14, respectively [19] were slightly higher than the clearing temperatures for the Pd-derivatives (120.5 °C, 103.9 °C and 98.9 °C, respectively, measured on the heating). Therefore, both the skeletal molecular characteristics and the packing arrangement observed for the Pd-derivatives seem to favour that they exhibit liquid crystal properties.

4. Concluding remarks

It has been established that in most cases the shape of the mesogen determines the symmetries of the resulting thermotropic mesophases. So, ellipsoidal molecules give rise to nematic and lamellar phases whereas discoid molecules display columnar mesomorphism [1]. In our Pd-complexes, the molecular structure indicate that these mesogens should be considered as rod-like type,

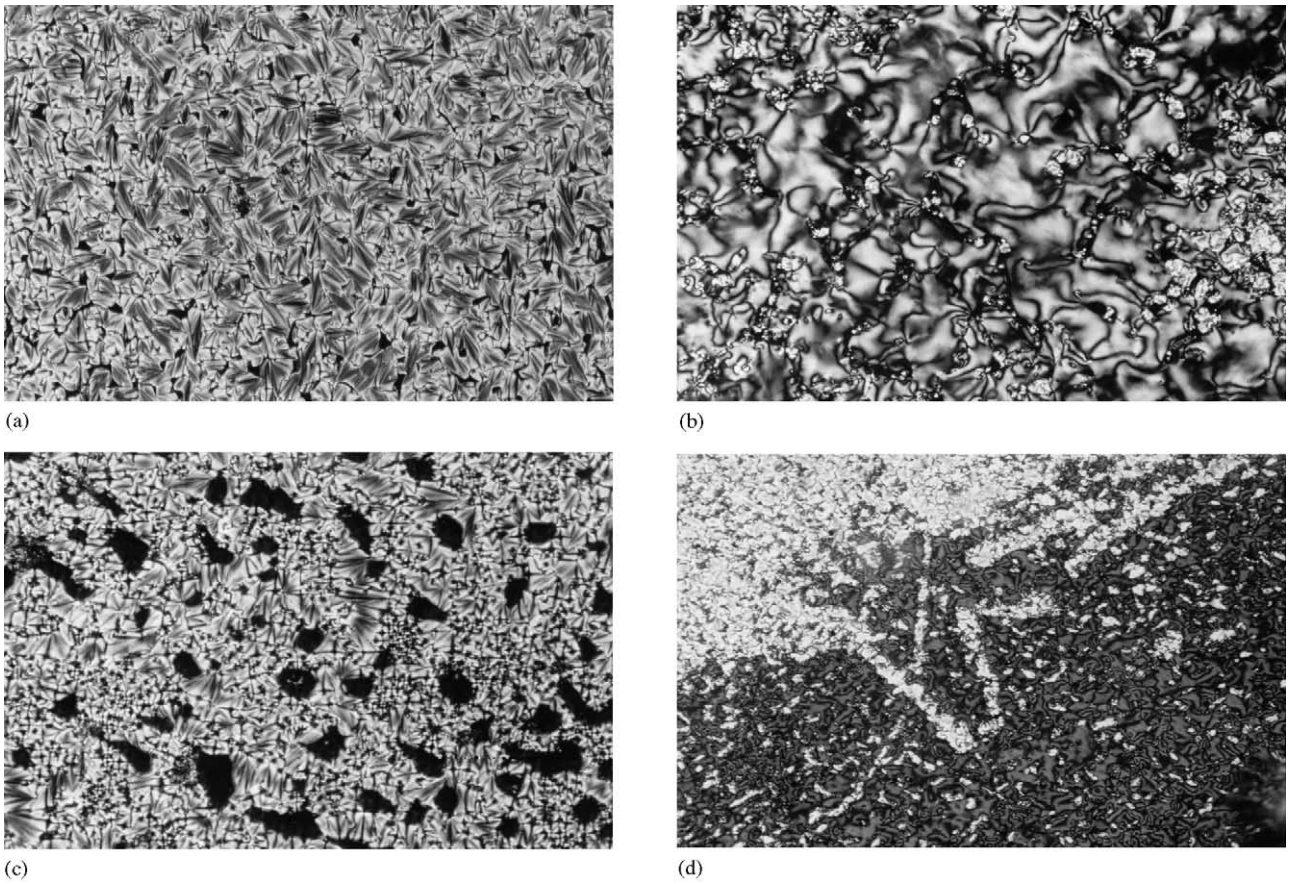

Fig. 5. Textures of the smectic mesophases on cooling of (a) **2** at 92.9 °C (SmA), (b) **5** at 80.6 °C (SmC), (c) **3** at 90.0 °C (SmA), and (d) **3** at 57.6 °C (SmC).

which is established on the basis of the overall molecular geometry as well as the molecular dimensionality determined by the position of the alkyloxy substituents (3 and 5) on the pyrazolate ligands and by the number of carbons (higher than 8). The arrangement of this type of rod-like molecules results preferentially in the formation of a layer-like structure in the solid state, and these Pd(II) complexes appear to arrange in a similar layered structure in the mesophases.

5. Supplementary material

Crystallographic data for the structural analysis have been deposited with the Cambridge Crystallographic Data Centre, CCDC No. 206256 for compound **3**. Copies of this information may be obtained free of charge from The Director, CCDC, 12 Union Road, Cambridge CB2 1EZ, UK (Fax: +44-1223-336033; e-mail: deposit@ccdc.cam.ac.uk or www: http://www.ccdc.cam.ac.uk).

Acknowledgements

Financial support from the DGES of Spain is gratefully acknowledged (Project No. PB98-0766).

References

[1] B. Donnio, D.W. Bruce, Struct. Bond. 95 (1999) 193.
[2] S.R. Collinson, D.W. Bruce, in: J.P. Sauvage (Ed.), Transition Metals in Supramolecular Chemistry (Chapter 7), Wiley, Chichester, 1999, pp. 285–369 (Chapter 7).
[3] J.L. Serrano (Ed.), Metallomesogens: Synthesis, Properties and Applications, VCH, New York, 1996.
[4] D.W. Bruce, Adv. Inorg. Chem. 52 (2001) 151.
[5] J. Malthête, A. Collet, New J. Chem. 9 (1985) 151.
[6] H. Zimmermann, R. Poupko, Z. Luz, J. Billard, Z. Naturfosch. A 40 (1985) 149.
[7] B. Xu, T.M. Swager, J. Am. Chem. Soc. 115 (1993) 1159 (and references therein).
[8] A. Jakli, A. Saupe, G. Scherowsky, X.H. Chen, Liq. Cryst. 22 (1997) 309.
[9] J. Billard, Liq. Cryst. 24 (1998) 99.
[10] R. de la Cruz, P. Espinet, A.M. Gallego, J.M. Martín-Alvarez, J.M. Martínez-Ilarduya, Polyhedron 663 (2002) 108 (and references therein).
[11] S. Trofimenko, Prog. Inorg. Chem. 34 (1986) 115.
[12] S. Trofimenko, Chem. Rev. 93 (1993) 943.
[13] G. La Monica, G.A. Ardizzoia, Prog. Inorg. Chem. 46 (1997) 151.
[14] L.A. Oro, M.A. Ciriano, C. Tejel, Pure Appl. Chem. 70 (1998) 779.
[15] A.P. Sadimenko, Adv. Heterocycl. Chem. 80 (2001) 157.
[16] S. Trofimenko, Inorg. Chem. 10 (1971) 1372.
[17] G.W. Henslee, J.D. Oliver, J. Cryst. Mol. Struct. 7 (1977) 137.
[18] Z. Wang, C.D. Abernethy, A.H. Cowley, J.N. Jones, R.A. Jones, C.L.B. Macdonald, L. Zhang, J. Organomet. Chem. 666 (2003) 35.
[19] M.C. Torralba, M. Cano, J.A. Campo, J.V. Heras, E. Pinilla, M.R. Torres, J. Organomet. Chem. 654 (2002) 150.
[20] M.C. Torralba, M. Cano, J.A. Campo, J.V. Heras, E. Pinilla, M.R. Torres, J. Organomet. Chem. 633 (2001) 91.
[21] M.A. Esteruelas, E. Sola, L.A. Oro, M.B. Ros, J.L. Serrano, J. Chem. Soc. Chem. Commun. (1989) 55.
[22] D.W. Bruce, D.A. Dunmur, M.A. Esteruelas, S.E. Hunt, R. Le Lagadec, P.M. Maitlis, J.R. Marsden, E. Sola, J.M. Stacey, J. Mater. Chem. 1 (1991) 251.
[23] M.C. Torralba, M. Cano, J.A. Campo, J.V. Heras, E. Pinilla, M.R. Torres, Inorg. Chem. Commun. 5 (2002) 887.
[24] K. Ohta, H. Muroki, K.I. Hatada, I. Yamamoto, K. Matsuzaki, Mol. Cryst. Liq. Cryst. 130 (1985) 249.
[25] J.A. Campo, M. Cano, J.V. Heras, M.C. Lagunas, J. Perles, E. Pinilla, M.R. Torres, Helv. Chim. Acta 84 (2001) 2316.
[26] J. Barberá, C. Cativiela, J.L. Serrano, M.M. Zurbano, Liq.Cryst. 11 (1992) 887.
[27] Siemens, SAINT: data collection and procedure software for the SMART system, Siemens Analytical X-ray Instrument, Inc., Madison, WI, 1995.
[28] Bruker, SHELXTL™, Version 6.1, Bruker Analytical X-ray Systems, 2000.
[29] E. Dowty, ATOMS for Windows 3.1: A computer program for displaying atomic structure, Kingsport, TN, 1995.
[30] M. Cano, J.V. Heras, M. Maeso, M. Alvaro, R. Fernández, E. Pinilla, J.A. Campo, A. Monge, J. Organomet. Chem. 534 (1997) 159.
[31] S. Trofimenko, J.C. Calabrese, J.K. Kochi, S. Wolowiec, F.B. Hulsbergen, J. Reedijk, Inorg. Chem. 31 (1992) 3943.
[32] N. Tsukada, T. Sato, H. Mori, S. Sugawara, C. Kabuto, S. Miyano, Y. Inoue, J. Organomet. Chem. 627 (2001) 121.
[33] C.P. Butts, J. Crosby, G.C. Lloyd-Jones, S.C. Stephen, Chem. Commun. (1999) 1707.
[34] P. Bhattacharyya, A.M.Z. Slawin, M.B. Smith, J. Chem. Soc. Dalton Trans. (1998) 2467.
[35] K. Tsutsumi, S. Ogoshi, S. Nishiguchi, H. Kurosawa, J. Am. Chem. Soc. 120 (1998) 1938.